

On the Post-Peak Structural Response due to Softening with Localization

Hui-Hui Dai *

Department of Mathematics
and Liu Bie Ju Centre
for Mathematical Sciences,
City University of Hong Kong,
83 TatChee Avenue,
Kowloon Tong, Hong Kong
Email: mahhdai@cityu.edu.hk
Tel: +852 27888660; fax: +852 27888561.

Xiaowu Zhu

School of Mathematics and Statistics,
Wuhan University, Wuhan 430072, P.R. China
Department of Mathematics,
City University of Hong Kong,
83 TatChee Avenue,
Kowloon Tong, Hong Kong

Zhen Chen

Department of Civil and Environmental Engineering,
University of Missouri-Columbia, Columbia, MO 65211-2200 USA
Department of Engineering Mechanics,
Dalian University of Technology,
Dalian 116024, P.R. China.

An analytical study is taken to investigate the relationship between material softening and structural softening through the use of a model problem in one dimension. With general nonlinear assumptions on the constitutive relations, it turns out that the governing equations can be viewed as a system of parametric equations, which couple the size effect and the nonlinear effect. Compared with the bilinear assumptions in previous literature, we find that the nonlinear assumptions herein capture more details in the post-peak structural response. After doing standard mathematical analysis to the nonlinear equations, we manage to derive necessary and sufficient conditions for the occurrence of four important post-peak cases, which are often observed in experiments. In particular, our analysis reveals that the mechanism of the snap-through phenomenon is due to the convexity change of the constitutive curve of the softening part. Mathematical examples are also given to illustrate the proposed procedures.

1 Introduction

Strain-softening, i.e., the decrease of stress with the increase of strain, is such a common phenomenon that has been recorded for a variety of materials, like concrete, rocks, ceramics, metals, etc. Bazant et al., [1] gave a comprehensive review of this phenomenon and analyzed its mechanism from a continuum point of view. Moreover, it is well-known that strain softening is always accompanied by highly localized

deformations of the specimen ([2, 3]). Due to the importance of softening phenomenon in structural safety assessment, many efforts have been made in the past decades to investigate strain-softening with localization experimentally, numerically, and analytically, as reviewed by [4, 5].

Snap-back may be one of the most interesting and perhaps most common structural instability phenomena observed in experiments. It shows that the load-displacement curve displays a positive slope after attaining the peak load. de Borst [6] demonstrated the possibility of snap-back behavior on structural level by means of two concrete structures: a reinforced concrete and an unreinforced specimen. In order to simulate the highly localized failure mode in a strain-softening solid, a modified arc-length control method was used in that paper. Later, Rots and de Borst [7] did a tensile test on concrete specimens and analyzed it by using the finite element method, with a particular attention on the snap-back behavior. He et al., [8] studied the class II behavior (snap-back) of rock with a spring model, which was characterized by non-uniform failure. Unloading-reloading tests were also conducted in the post failure region in that paper. One of their results is that, if inelastic strain increases slower than the elastic strain decreases, rock shows class II behavior.

Jansen et al. [9] did an experiment on concrete cylinders by using the feedback-control method. From two test series, the stress-displacement behavior for different height-diameter ratios with normal strength and high strength were

obtained. They found that the pre-peak segment of the stress-displacement curves agrees well with the pre-peak part of the stress-strain curves, while the post-peak segment shows a strong dependence on the geometric size, namely the radius-length ratio. More specifically, the longer the specimen is, the steeper the post-peak segment of the stress-displacement curves becomes. The feedback-control method was also used in Subramaniam et al. [10] to test concrete in torsion, and snap-back was also found in the experiment.

Some analytical studies were also taken to investigate softening with localization. With the use of a one-dimensional model, Schreyer and Chen [11] analyzed the snap-back phenomenon and found the important size effect on the instability. Due to the simplicity of bilinear assumptions on the constitutive relations, further features like snap-through were lost in the result, although in some experiments this feature was observed (see van Vilet and van Mier [12]). The same constitutive relations were also assumed in Chen et al. [13] to analyze the stability in some hierarchical structures. In a more complex setting with certain nonlinear assumptions on the constitutive relations, Sundara Raja Iyengar et al. [14] took an analytical study. By using the fictitious crack model (FCM) developed by Hillerborg, they found the effect of the softening exponent n on the size effect and snap-back behavior of beams, while the stress-displacement relation was assumed as a general power law function. Dai et al. [15] constructed the analytical solutions for localizations in a hyperelastic slender cylinder. With the use of coupled series-asymptotic expansions approach and phase plane analysis, they solved the partial differential equations and found that the width of the localization zone depends on the material parameters in the post-peak region. Further, they showed that there is a snap-back phenomenon when the radius-length ratio is relatively small, which agrees well with experimental observations. Dai et al. [16] showed a similar result for hyperelastic shape memory alloys. Gradient theory may be another powerful tool in dealing with localization of deformation (see Triantafyllidis and Aifantis [17]). For example, Triantafyllidis and Bardenhagen [18] investigated the issues of instability and imperfection sensitivity of the solutions of a boundary value problem in one dimension. Their results also revealed some important size effect.

To the authors' knowledge, however, there is not any analytical study with general nonlinear constitutive relations in the open literature which explores the role played by the convexity of the constitutive curve of the softening part and the coupling effect between this convexity and the size. Also, both snap-back and snap-through were observed in some experiments, but no analytical results are available for explaining the transition from snap-back to snap-through. We shall explore these aspects in this paper. To gain insight into the post-peak response, we study the same one-dimensional structure as considered in [11, 19, 20, 21]. The difference is that here we use general nonlinear constitutive relations, instead of the bilinear ones used in these papers. First, we set up the stress-strain equations for the structure in the post-peak region, which are nonlinear as compared with the bilinear case. After some analysis, we derive the mathemati-

cal conditions for the occurrence of several important curves as frequently observed in experiments, including the snap-through (which cannot be captured by the bilinear assumptions). Finally, an example is given to illustrate these cases, and the post-peak curves are consistent with our theoretical predictions.

2 Model Problem

To simulate post-peak experiments, we consider a structure with a serial arrangement of intact elastic and strain-softening zones. This model was used by several researchers, such as [19, 20, 21] in the early years. In [11], it was introduced to analyze strain-softening with bilinear assumptions on the constitutive relations. As shown in Figure 1(a), the structure is a bar of length $L = a + b$ with a unit cross-sectional area. That is to say, it is composed of two segments (segment A with length a and segment B with length b). The two segments are usually described by similar constitutive equations, and the main difference is that the limit stress for B is slightly less than that of A. Therefore, if the stress on the structure is such that the strain in region B exceeds the value at the limit state, then softening will occur. It is assumed that softening occurs uniformly over a localized region B under quasi-static loading.

In order to consider a general nonlinear case, the constitutive relations for the two regions are set as: the loading and unloading segments of region A are two arbitrary functions f_{11} and f_{12} respectively, while the loading and softening segments of region B are two arbitrary functions f_{21} and f_{22} respectively. Moreover, we assume that the foregoing nonlinear functions are twice differentiable with $f'_{11} > 0$, $f'_{12} > 0$, $f'_{21} > 0$, $f'_{22} < 0$. The limit stress for region A, denoted by σ_a , is assumed to be slightly larger than that of region B, which is denoted by σ_0 . The details are shown in Figure 1(b) (where f_1 is used to denote both the pre-peak and the post-peak segments, as region A only experiences loading or unloading). As the post-peak curve of the structure is our main concern, in the following derivation, for simplicity, we use f_1 , f_2 to denote the post-peak curves of region A and region B respectively, unless otherwise specified.

As to the post-peak response, for a strain softening material with a serial setting (cf. Figure 1(a)), region A is in an unloading process and region B experiences strain softening. Given the values of strain in regions A and B, say e_1 and e_2 , respectively, then the composite strain for the complete structure is given by

$$e = \frac{ae_1 + be_2}{L} = (1 - n)e_1 + ne_2, \quad (1)$$

where $n = b/L$. Since we consider it as a quasi-static problem, the composite stress is then given by

$$\sigma = f_1(e_1) = f_2(e_2). \quad (2)$$

In fact, one can easily see that (1) and (2) are also true if

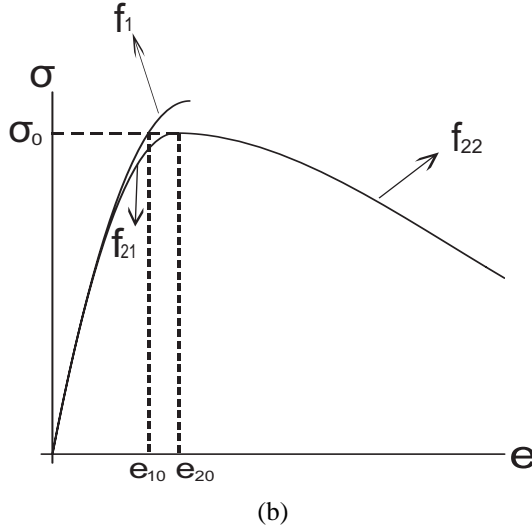
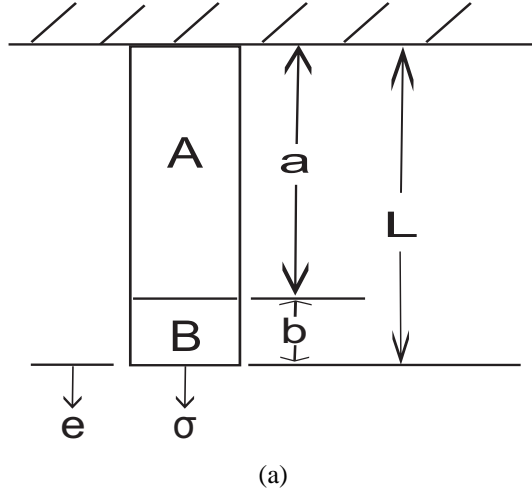


Fig. 1. (a) One-dimensional model problem; (b) Stress-strain relations for A and B.

f_2 is used to denote both the pre-peak and post-peak segments. Here, for the post-peak region, we consider only when $\sigma \geq \sigma^*$ (σ^* represents the lowest stress value at which the bar breaks), and denote e_{11} and e_{21} the values such that $f_1(e_{11}) = f_2(e_{21}) = \sigma^*$. Then, for the post-peak region, we have $e_1 \in [e_{11}, e_{10}]$ and $e_2 \in [e_{20}, e_{21}]$ (see Figure 1(b) for the definitions of e_{10} and e_{20}). From equation (2), we get $e_2 = f_2^{-1}[f_1(e_1)]$ (or $e_1 = f_1^{-1}[f_2(e_2)]$). Thus (1) and (2) can be transformed into the system

$$\begin{cases} \sigma = f_1(e_1) \\ e = (1-n)e_1 + nf_2^{-1}[f_1(e_1)], \end{cases} \quad (3)$$

which can be viewed as the parametric equations for the engineering stress-strain curve. We note that n is actually the width (scaled by L) of the localization zone in the reference configuration, as material points in region B are in the localization zone in the post-peak region. Obviously, system (3) couples the size effect and nonlinear effect.

Now, we differentiate system (3) with respect to e_1 to

obtain

$$\begin{cases} \frac{d\sigma}{de_1} = f_1'(e_1) \\ \frac{de}{de_1} = (1-n) + n\frac{f_1'(e_1)}{f_2'(e_2)}. \end{cases} \quad (4)$$

If $(1-n)f_2'(e_2) + nf_1'(e_1) \neq 0$, we have

$$\frac{d\sigma}{de} = \frac{f_1'(e_1)f_2'(e_2)}{(1-n)f_2'(e_2) + nf_1'(e_1)}, \quad (5)$$

$$\frac{d^2\sigma}{de^2} = \frac{n[f_1'(e_1)]^3 f_2''(e_2) + (1-n)f_1''(e_1)[f_2'(e_2)]^3}{[nf_1'(e_1) + (1-n)f_2'(e_2)]^3}. \quad (6)$$

In order to analyze the sign of (5), we define

$$g(e_1, e_2; n) = nf_1'(e_1) + (1-n)f_2'(e_2), \quad (7)$$

$$m(e_1, e_2) = \frac{f_2'(e_2)}{f_2'(e_2) - f_1'(e_1)}, \quad (8)$$

$$G(e_1, e_2) = [f_1'(e_1)]^2 f_2''(e_2) - [f_2'(e_2)]^2 f_1''(e_1). \quad (9)$$

The above three functions can be viewed as functions of either e_1 or e_2 by the relations between them as shown above. We note that $m(e_1, e_2)$ depends on the slopes (the first-order derivatives) of the constitutive curves, $G(e_1, e_2)$ depends on the convexities (the second-order derivatives) of the constitutive curves and $g(e_1, e_2; n)$ depends on the size parameter n . We also point out that $m(e_1, e_2) = n$ is equivalent to $g(e_1, e_2; n) = 0$. We shall see that n has an important influence on the structural response.

3 Post-peak Curves and Conditions

Assuming that $f_2'(e_{20}) = 0$ and $f_2''(e_{20}) < 0$, that is to say e_{20} is a local maximum of f_2 . Then, for different f_1 , f_2 and n the four cases shown in Figure 2 can arise. Next, we shall establish the conditions for each case.

3.1 Case A: Stable Softening

For the structure to be in stable softening (i.e., $d\sigma/de < 0$), from (5), it is easy to see the necessary and sufficient condition is

$$g(e_1, e_2; n) = nf_1'(e_1) + (1-n)f_2'(e_2) > 0, \text{ for } e_1 \in [e_{11}, e_{10}]. \quad (10)$$

From which, we get

$$\frac{b}{L} = n > n_0 := \max_{e_1 \in [e_{11}, e_{10}]} m(e_1, e_2) = \max_{e_2 \in [e_{20}, e_{21}]} m(e_1, e_2). \quad (11)$$

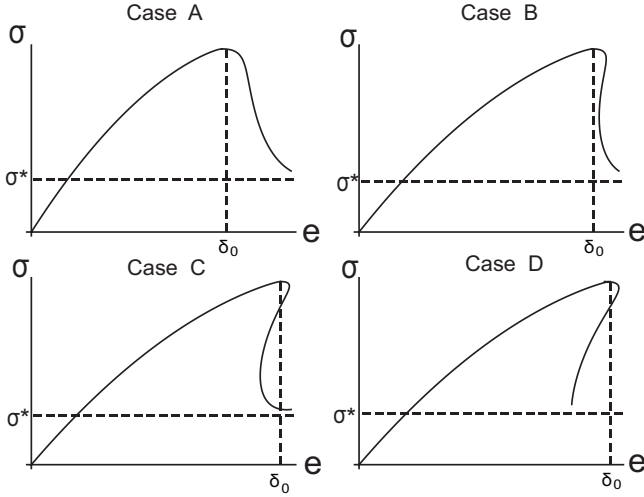


Fig. 2. Four cases of the post-peak engineering stress-strain curves

3.2 Cases B and C: Snap-Through

Now, we focus on the interval $n \in (0, n_0]$. There are several possibilities, as shown in Figure 2. Before analyzing the remaining cases, we point out that the initial part (i.e., the part close to the peak) of the post-peak curve is in a state of stable softening for the conditions imposed on f_1 and f_2 . In fact, $g(e_{10}, e_{20}) = n f_1'(e_{10}) > 0$, and at the peak point, we have $d\sigma/de < 0$. By continuity, there must be a part of the post-peak curve for e close to δ_0 ($\delta_0 = (1-n)e_{10} + ne_{20}$) in which $d\sigma/de < 0$. Also, at $e_1 = e_{10}, e_2 = e_{20}$, we have $d^2\sigma/de^2 = f_2''(e_{20})/n^2 < 0$. This would be useful for our later derivation.

We see that each of Case B and Case C represents a snap-through case. Here, snap-through is defined to be the point at which the slope of the force-displacement curve becomes infinite. As a result, when displacement (elongation) crosses this point, the force may experience a sudden drop. Firstly, let us consider the similarities between Case B and Case C. There are two turning points (the points at which $d\sigma/de = \infty$) in both curves. From (5), it can be seen that this is equivalent to that the equation

$$g(e_1, e_2; n) = n f_1'(e_1) + (1-n) f_2'(e_2) = 0 \quad (12)$$

has two roots, say e_{11}^* and e_{12}^* ($e_{11}^* > e_{12}^*$). The following theorem provides a necessary and sufficient condition for the occurrence of the two turning points.

Theorem 3.1. *If two turning points occur, then the function $G(e_1, e_2)$ must change sign at least once for $e_1 \in [e_{11}, e_{10}]$. On the other hand, if the sign of $G(e_1, e_2)$ changes only once for $e_1 \in [e_{11}, e_{10}]$, then for any $n \in [n_1, n_0]$, two turning points occur; where $n_1 = m(e_{11}, e_{21})$.*

Proof. If two turnings occur, then the sign of the function $g(e_1, e_2)$ changes twice (cf. Case B or Case C in Figure 2).

So, we get

$$g(e_{11}, e_{21}; n) = n f_1'(e_{11}) + (1-n) f_2'(e_{21}) > 0. \quad (13)$$

Thus,

$$\frac{f_2'(e_{21})}{f_1'(e_{11})} > -\frac{n}{1-n}. \quad (14)$$

Since

$$-\frac{n}{1-n} \geq -\frac{n_0}{1-n_0}, \quad (15)$$

$$-\frac{n_0}{1-n_0} = \min_{e_1 \in [e_{11}, e_{10}]} \frac{f_2'(e_2)}{f_1'(e_1)}, \quad (16)$$

we have

$$\frac{f_2'(e_{21})}{f_1'(e_{11})} > \min_{e_1 \in [e_{11}, e_{10}]} \frac{f_2'(e_2)}{f_1'(e_1)}. \quad (17)$$

Suppose that the minimum is attained at e_{12} (the corresponding e_2 is given by $f_2^{-1}[f_1(e_{12})] = e_{22}$). That is, $f_2'(e_{22})/f_1'(e_{12}) = \min_{e_1 \in [e_{11}, e_{10}]} \{f_2'(e_2)/f_1'(e_1)\}$. If we view

$f_2'(e_2)/f_1'(e_1)$ as a function of e_2 , then according to the Lagrange Mean Value theorem, there exists an $\xi \in (e_{22}, e_{21})$ such that

$$\frac{d}{de_2} \left[\frac{f_2'(e_2)}{f_1'(e_1)} \right]_{e_2=\xi} = \frac{\frac{f_2'(e_{21})}{f_1'(e_{11})} - \frac{f_2'(e_{22})}{f_1'(e_{12})}}{e_{21} - e_{22}} > 0. \quad (18)$$

As

$$\frac{d}{de_2} \left[\frac{f_2'(e_2)}{f_1'(e_1)} \right] = \frac{[f_1'(e_1)]^2 f_2''(e_2) - [f_2'(e_2)]^2 f_1''(e_1)}{[f_1'(e_1)]^3}, \quad (19)$$

we have

$$[f_1'(\zeta)]^2 f_2''(\xi) - [f_2'(\xi)]^2 f_1''(\zeta) > 0, \text{ where } \zeta = f_1^{-1}[f_2(\xi)], \quad (20)$$

which implies that $G(\zeta, \xi) > 0$. Since $G(e_{10}, e_{20}) = [f_1'(e_{10})]^2 f_2''(e_{20}) < 0$, the sign of $G(e_1, e_2)$ changes for $e_1 \in [e_{11}, e_{10}]$.

On the other hand, suppose that for $e_1 \in [e_{11}, e_{10}]$, $G(e_1, e_2)$ changes sign once. Now, we consider the function $m(e_1, e_2)$ (cf., (8); we regard it as a function of e_2). We now

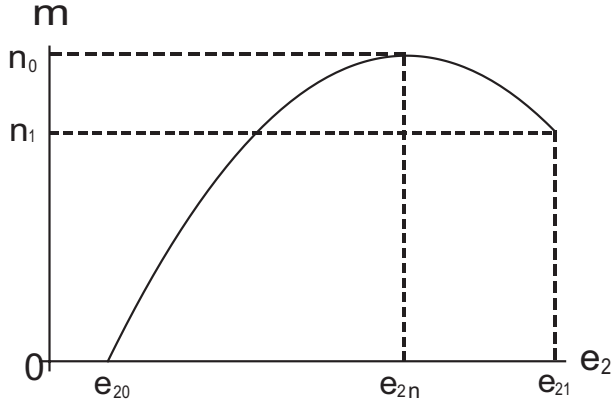


Fig. 3. Schematic illustration of $m(e_1, e_2)$

show that for any $n \in [n_1, n_0]$, equation (12) has two roots. In fact, it is easy to get

$$\frac{dm}{de_2} = \frac{-G(e_1, e_2)}{[f_2'(e_2) - f_1'(e_1)]^2 f_1'(e_1)}. \quad (21)$$

Thus, dm/de_2 also changes sign once. We also note that n_0 is a maximum of $m(e_1, e_2)$, say, attained at e_{2n} . Then, $dm/de_2 = 0$ at $e_2 = e_{2n}$. On the other hand,

$$\left. \frac{dm}{de_2} \right|_{e_2=e_{20}} = \frac{-G(e_{10}, e_{20})}{[f_2'(e_{20}) - f_1'(e_{10})]^2 f_1'(e_{10})} > 0. \quad (22)$$

So, the curve $m(e_1, e_2)$ should have the characteristics shown in Figure 3. Thus, for any $n \in [n_1, n_0]$, $n = m(e_1, e_2)$ has two roots, which then implies that $g(e_1, e_2; n)$ has two zeros. This completes the proof of the second part of the theorem.

If f_1 is linear in the post-peak region, then $G(e_1, e_2) = [f_1'(e_1)]^2 f_2''(e_2)$. Consequently, the sign of $G(e_1, e_2)$ depends on the convexity of f_2 . We have the following corollary:

Corollary 3.1. *For f_1 being linear in the post-peak region, if two turning points occur, then the convexity of f_2 must change at least once for $e_1 \in [e_{11}, e_{10}]$. On the other hand, if the convexity of f_2 changes once, then for any $n \in [n_1, n_0]$, two turning points occur in the post-peak curve.*

Remark 3.1. *Usually, $f_{12}''(e_1)$ should be small ($f_{12}''(e_1) = 0$ for f_1 being linear). Thus, the sign of $G(e_1, e_2)$ is primarily determined by the sign of $f_{22}''(e_2)$. So, one may say that a necessary condition for the snap-through (i.e., there are two turning points in the post-peak curve) is the change of the convexity of the constitutive curve of the softening part.*

Now, let us consider the differences between Case B and Case C. Recall that e_{11}^* and e_{12}^* ($e_{11}^* > e_{12}^*$) are the two roots of equation (13). For Case B, we have

$$\delta_2^* = (1-n)e_{12}^* + nf_2^{-1}[f_1(e_{12}^*)] > \delta_0. \quad (23)$$

While for Case C, we have

$$\delta_2^* = (1-n)e_{12}^* + nf_2^{-1}[f_1(e_{12}^*)] \leq \delta_0. \quad (24)$$

In other words, in Case C the post-peak curve has entered the pre-peak region, while in Case B it has not. We find that, for given f_1 and f_2 , there are some conditions for the occurrence of Case C. For simplicity, we assume that the sign of $G(e_1, e_2)$ changes once, say,

$$\begin{cases} G(e_1, e_2) < 0, e_2 \in [e_{20}, e_{22}), \\ G(e_{12}, e_{22}) = 0, \\ G(e_1, e_2) > 0, e_2 \in (e_{22}, e_{21}]. \end{cases} \quad (25)$$

The following theorem provides a necessary and sufficient condition for Case C.

Theorem 3.2. *Under assumption (25) and $n \in [n_1, n_0]$, a necessary and sufficient condition for the occurrence of Case C is*

$$f_2'(e_{22}^*)(e_{22}^* - e_{20}) \geq f_1'(e_{12}^*)(e_{12}^* - e_{10}). \quad (26)$$

Proof. From (24), we have

$$(1-n)e_{12}^* + ne_{22}^* \leq (1-n)e_{10} + ne_{20}, \text{ where } e_{22}^* = f_2^{-1}[f_1(e_{12}^*)]. \quad (27)$$

On the other hand,

$$g(e_{12}^*, e_{22}^*; n) = nf_1'(e_{12}^*) + (1-n)f_2'(e_{22}^*) = 0. \quad (28)$$

From the above two equations, we can get (26) immediately. Also, from (26) and (28) one can immediately deduce (27). This completes the proof.

Assumption (25) can be made even more complicated, in that case we may draw the fairly complicated post-peak curves in [7], which were obtained by numerical methods. It should be pointed out that inequality (26) is another requirement among f_1 , f_2 and n . For given f_1 and f_2 , it provides another bound (say n_2) for n , since e_{22}^* and e_{12}^* are related to n as equation (28) shows.

For f_1 being linear in the post-peak region, it is easy to show that (26) becomes

$$f_2'(e_{22}^*) \geq \frac{f_2(e_{22}^*) - f_2(e_{20})}{e_{22}^* - e_{20}}. \quad (29)$$

This implies that for the constitutive relation $\sigma = f_2(e_2)$, the secant line joining the point e_{22}^* and the peak e_{20} should be steeper than the tangent line at e_{22}^* (see Figure 4). Combined with Corollary 3.1, we have the following corollary:

Corollary 3.2. *For f_1 being a linear function, if the convexity of f_2 changes once, then a necessary and sufficient condition for the occurrence of Case C is $n \in [n_1, n_0]$, and inequality (29) holds.*

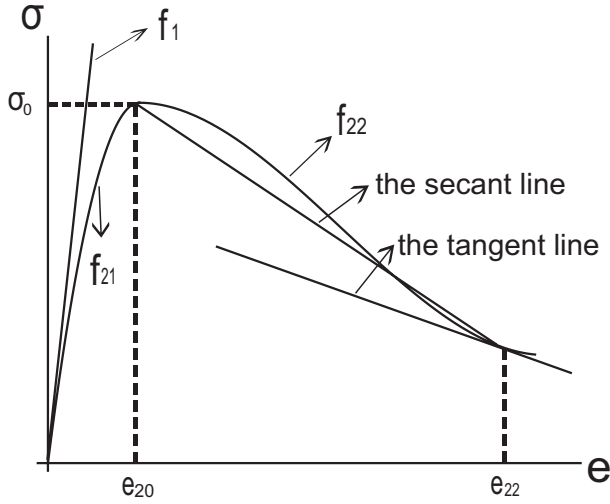


Fig. 4. Diagrammatic representation of inequality (29)

3.3 Case D: Snap-back

In Case D, there is a snap-back in the structural response. Here, we say that snap-back occurs when the slope of the force-displacement curve becomes positive and remains positive in the post-peak response. Obviously, in this case there is only one turning point (see Figure 2). The following theorem provides a critical n for the occurrence of Case D.

Theorem 3.3. *If $G(e_1, e_2)$ changes sign once (cf.(25)) or does not change sign for $e_1 \in [e_{11}, e_{10}]$, then for Case D to occur, a necessary and sufficient condition is $n < n_1$.*

Proof. First, suppose that $G(e_1, e_2)$ changes sign once. Then $m(e_1, e_2)$ has the characteristics shown in Figure 3. It is obvious that a necessary and sufficient condition for the occurrence of Case D is that there exists only one root for equation (12). While from Figure 3, it is easy to see that a necessary and sufficient condition is $n < n_1$. Second, suppose that $G(e_1, e_2)$ does not change sign. Since $dm/de_2 > 0$ (as $dm/de_2 > 0$ at $e_2 = e_{20}$), we have

$$n_0 = \max_{e_2 \in [e_{20}, e_{21}]} m(e_1, e_2) = m(e_{11}, e_{21}) = n_1. \quad (30)$$

Obviously, a necessary and sufficient condition for $n = m(e_1, e_2)$ to have one and only one root (i.e., $g(e_1, e_2; n)$ has one and only one zero) is $n < n_1$. Thus we complete the proof.

Remark 3.2. *In this section, we derive some requirements on the constitutive functions, together with three critical values (n_0, n_1, n_2) of the size parameter. Providing the constitutive requirements are met, the structural response may have different behaviors for n in different intervals according to the above critical values. Thus, the results also show the important size effects.*

4 Illustrative Examples

In this section, we give two examples to illustrate the theoretical results obtained in Section 3. The following two examples can be referred to as two different physical processes. One can easily check that the functions in the following examples satisfy the conditions we have proposed, in particular, (25).

Example 1: Consider the following constitutive relations:

$$f_{11}(e_1) = \csc \frac{9\pi}{20} \sin(50\pi e_1),$$

$$f_{12}(e_1) = (50\pi \csc \frac{9\pi}{20})e_1 - \frac{9\pi}{20} \csc \frac{9\pi}{20} + 1,$$

$$f_{21}(e_2) = \sin(50\pi e_2),$$

$$f_{22}(e_2) = 65625 \left[\frac{1}{3}(e_2 - 0.03)^3 - 0.0004(e_2 - 0.03) \right] + 0.65.$$

Here $\sigma_0 = 1$, and we take $\sigma^* = 0.301$. The details are shown in Figure 5(a).

We have taken f_{12} being a linear function, which represents the physical situation that at the peak region A of the structure has entered the plastic state. We find the critical values of n based on the theoretical analysis in Section 3: $n_0 = 0.142$, $n_1 = 0.0158$, $n_2 = 0.110$ (a bound for n found from inequality (29)). Specifically, Case A occurs if $n > 0.142$; Case B occurs if $0.110 < n \leq 0.142$; Case C occurs if $0.0158 \leq n \leq 0.110$; Case D occurs if $n < 0.0158$. Accordingly, by taking n to be in different intervals, we get the four cases as we have predicted in Section 3. They are shown in Figure 5(b).

To reflect the size effect on the localization zone, curves of the width of the localization zone in the current configuration versus the total elongation are shown in Figure 6. This width is denoted by d , whose expression is given by $d = n(1 + e_2)$. Here, for the purpose of clearness, we have used different scales for different curves. It can be seen that this width increases slowly in the pre-peak region and increases rapidly in the post-peak region. For the stable softening case ($n = 0.167$), there is only one value of d for a given e . For the snap-back case ($n = 0.0156$), there are two values of d for a given e . Also, d increases very fast, as e decreases in the post-peak region. For the two snap-through cases ($n = 0.1$ and $n = 0.125$), there are three values of d for e in some intervals. Thus, d may jump from a small value to a large value for e in these intervals, i.e., the localization zone may suddenly widen. Thus, the size parameter n has an important influence on the localization zone.

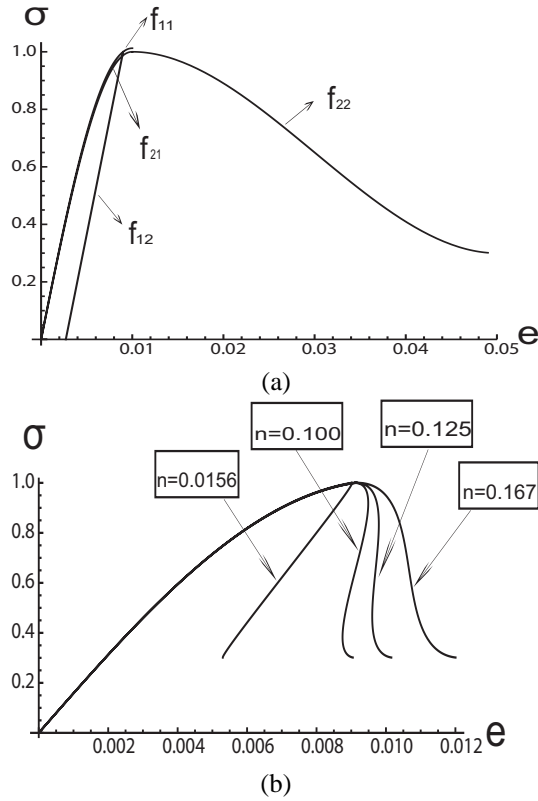


Fig. 5. (a) The constitutive curves of Example 1; (b) The engineering stress-strain curves for different n in Example 1.

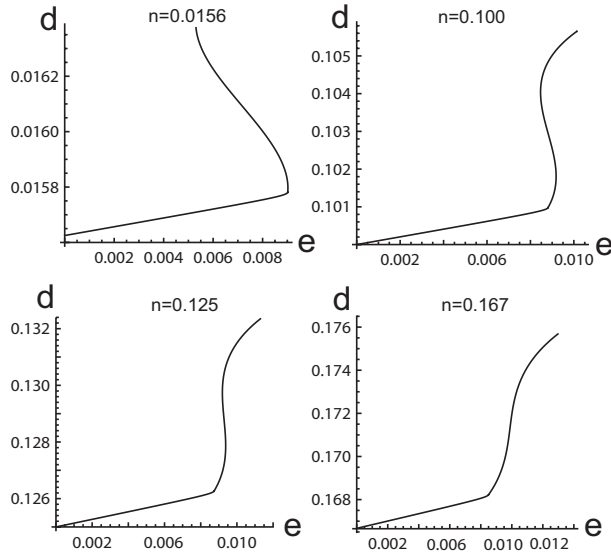


Fig. 6. The $d - e$ curves for different n in Example 1

Example 2: In this example, region A is assumed to be in nonlinear elasticity (loading or unloading), so the constitutive functions f_{11} and f_{12} are the same. The constitutive relations are listed below.

$$f_{11}(e_1) = f_{12}(e_1) = -11000(e_1 - 0.01)^2 + 1.1,$$

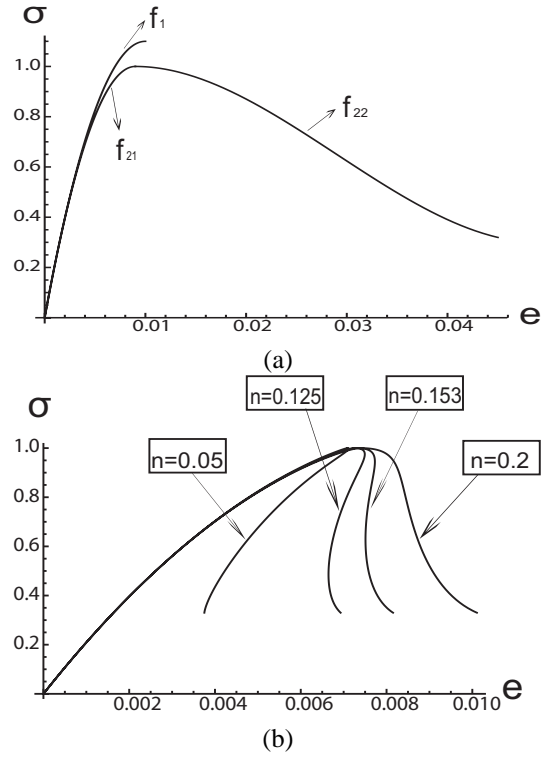


Fig. 7. (a) The constitutive curves of Example 2; (b) The engineering stress-strain curves for different n in Example 2.

$$f_{21}(e_2) = -\frac{10^6}{81}(e_2 - 0.009)^2 + 1,$$

$$f_{22}(e_2) = 65625\left[\frac{1}{3}(e_2 - 0.029)^3 - 0.0004(e_2 - 0.029)\right] + 0.65.$$

Here $\sigma_0 = 1$, and we take $\sigma^* = 0.333$. The details are shown in Figure 7(a). Critical values of n are: $n_0 = 0.174$, $n_1 = 0.0614$, $n_2 = 0.136$ (a bound for n found from inequality (26)). The intervals for different cases are: Case A occurs if $n > 0.174$; Case B occurs if $0.136 < n \leq 0.174$; Case C occurs if $0.0614 \leq n \leq 0.136$; Case D occurs if $n < 0.0614$. The curves for n taking four values in these four different intervals are shown in Figure 7(b), which agree with our theoretical predictions in Section 3. Curves of the width of the localization zone in the current configuration versus the total elongation are also shown (see Figure 8). Once again, from these curves, one can see the important influence of the size parameter n on the localization zone.

5 Concluding Remarks and Future Tasks

An analytical study is performed on the post-peak structural response of strain-softening with localization. In a general nonlinear setting, after taking standard mathematical analysis to the parametric equations, we manage to handle the nonlinear and size effects. Qualitative requirements on the constitutive functions and quantitative requirements on the size effect are derived, especially for the snap-through

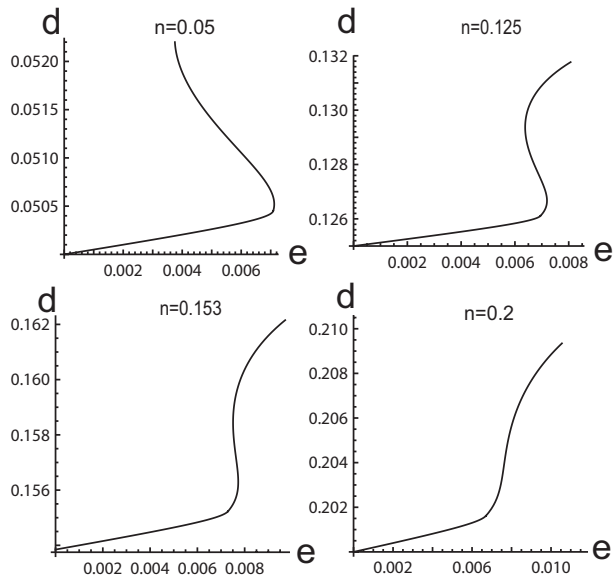


Fig. 8. The $d - e$ curves for different n in Example 2

phenomenon. The results are consistent with earlier experimental and computational results. It seems that the four cases studied analytically here are quite representative. The theoretical results may be of value for the verification of computational algorithms and can shed some light on the mechanisms of instabilities associated with strain-softening. Especially, we have shown that the convexity change is a necessary condition for the snap-through phenomenon. As softening with localization is important for understanding the failure evolution in structures, future work will focus on considering structures with different configurations.

Acknowledgement

The work described in this paper is supported by a grant from City University of Hong Kong (Project No. 7002366), the National Natural Science Foundation of China (Nos. 10721062, 90715037, 10728205 and 10902021), the Program for Changjiang Scholars and Innovative Research Team in University of China (PCSIRT), the 111 Project (No. B08014) and the National Key Basic Research Special Foundation of China (No. 2010CB832704).

References

[1] Bazant, Z.P., Belytschko, T.B., Ta-Peng Chang, 1984, "Continuum Theory for Strain-Softening," *Journal of Engineering Mechanics*, 110(12), 1666-1692.

[2] van Mier, J.G.M., 1986, "Fracture of Concrete under Complex Stress," *HERON*, 31(3).

[3] Read, H.E. and Hegemier, G.A., 1984, "Strain-softening of Rock, Soil and Concrete-A Review Artical," *Mechanics of Materials*, 3, 271-294.

[4] Bazant, Z.P., and Chen, E.P., "Scaling of Structure Failure, *Applied Mechanics Reviews*," 1997, 50, 593-627.

[5] Labuz, J. F., and Biolzi, L., 2007, "Experiments with

Rock: Remarks on Strength and Stability Issues," *International Journal of Rock Mechanics and Mining Sciences*, 44, 525-537.

[6] de Borst, R., 1987, "Computation of Post-bifurcation and Post-failure Behavior of Strain-softening solids," *Computers & Structures*, 25, 211-224.

[7] Rots, J.G., de Borst, R., 1989, "Analysis of Concrete Fracture in "Direct" Tension," *International Journal of Solids and Structures*, 25(12), 1381-1394.

[8] He, C., Okubo, S., and Nishimatsu, Y., 1990, "A Study on the Class II Behavior of Rock," *Rock Mechanics and Rock Engineering*, 23, 261-273.

[9] Jansen, D.C., Shah, S.P., 1997, "Effect of Length on Compressive Strain Softening of Concrete," *Journal of Engineering Mechanics*, 123, 25-35.

[10] Subramaniam, K.V., Popovics, J.S., Shah, S.P., 1998, "Testing Concrete in Torsion: Instability Analysis and Experiments," *Journal of Engineering Mechanics*, 124(11), 1258-1268.

[11] Schreyer, H. L., Chen, Z., 1986, "One-Dimensional Softening with Localization," *Journal of Applied Mechanics*, 53, 791-797.

[12] van Vilet, M.R.A., van Mier, J.G.M., 2000, "Experimental Investigation of Size Effect in Concrete and Sandstone under Uniaxial Tension," *Engineering Fracture Mechanics*, 65, 165-188.

[13] Chen, Z., Gan, Y., Labuz, J.F., 2008, "Analytical and Numerical Study of the Size Effect on the Failure Response of Hierarchical Structures," *International Journal for Multiscale Computational Engineering*, 6(4), 339-348.

[14] Sundara Raja Iyengar, K.T., Raviraj, S., Jayaram, T.N., 2002, "Analysis of Crack Propagation in Strain-Softening Beams," *Engineering Fracture Mechanics*, 69, 761-778.

[15] Dai, H.-H., Hao, Yanhong, Chen, Z., 2008, "On Constructing the Analytical Solutions for Localization in a Slender Cylinder Composed of an Incompressible Hyperelastic Material," *International Journal of Solids and Structures*, 45(9), 2613-2628.

[16] Dai, H.-H., Wang, Jiong, Chen, Z., 2009, "An analytical study of the instability of a superelastic shape memory alloy cylinder subject to practical boundary conditions," *Smart Matererials and Structures*, 18.

[17] N.Triantafllidis and E.C. Aifantis, 1986, "A Gradient Approach to Localization Deformation I. Hyperelastic Materials," 16, *Journal of Elasticity*, 225-237.

[18] N.Triantafllidis and S.Bardenhagen, 1993, "On Higher Order Gradient Continuum Theories in 1-D Nonlinear Elasticity. Derivation from and Comparison to the corresponding Discrete Models," 33(3), *Journal of Elasticity*, 259-293.

[19] Willam, K.J., Pramono, E., and Sture, S., 1985, "Stability and Uniqueness of Strain-Softening Computations," *Structural Research Series 8503*, Department of Civil, Environmental and Architectural Engineering, University of Colorado, Boulder.

[20] Crisfield, M.A., 1982, "Local Instabilities in the Non-

linear Analysis of Reinforced Concrete Beams and Slabs,” Proceedings of the Institution for Civil Engineers, 73(12), 135-145.

- [21] Schreyer, H. L., Chen, Z., 1984, “The Effect of Localization on the Softening Behavior of Structure Members,” Proceedings of the Symposium on Constitutive Equations: Micro, Macro, and Computational Aspects, Willam, K., ed., ASME Winter Annual Meeting, New Orleans, 10-14, Dec. 1984, 193-203.